ACS OMEGA

Open Access

http://pubs.acs.org/journal/acsodf

Article

Investigating the *Taenia solium* Fatty Acid Binding Protein Superfamily for Their Immunological Outlook and Prospect for Therapeutic Targets

Suraj S. Rawat, Gagandeep Singh, and Amit Prasad*

Cite This: *ACS Omega* 2024, 9, 22557−22572

Read Online

ACCESS | Metrics & More | Article Recommendations | Supporting Information

ABSTRACT: *Taenia solium*, like other helminthic parasites, lacks key components of cellular machinery required for endogenous lipid biosynthesis. This deficiency compels the parasite to obtain all of its lipid requirements from its host. The passage of lipids across the cell membrane is tightly regulated. To facilitate effective lipid transport, the cestode parasite utilizes certain lipid binding proteins called FABPs. These FABPs bind with the lipid ligands and allow the transport of lipids across the membranes and into the cytosol. Here, by integrating a computational with homology protein prediction tools, we had identified five FABPs in the *T. solium* proteome. We confirmed their presence by RNA expression analysis of respective genes from the parasite's cysticerci transcript. During the molecular modeling and MD simulation studies, two of them, TsM_000544100 and TsM_001185100, were most stable. Furthermore, they had a robust interaction with the IgG1 molecule, as evidenced by MD simulation. In addition, by employing *in silico* screening, we had identified potential ligand interacting residues that are present on the probable druggable site. In combination with *in vitro* cysticidal assays, enalaprilat dihydrate showed efficacy against cysticerci, which suggests that FABPs play a significant role in the cysticercus life cycle. Together, we provided a detailed distribution of all FABPs expressed by *T. solium* cysticerci and the critical role of TsM_001185100 in cysticercus viability.

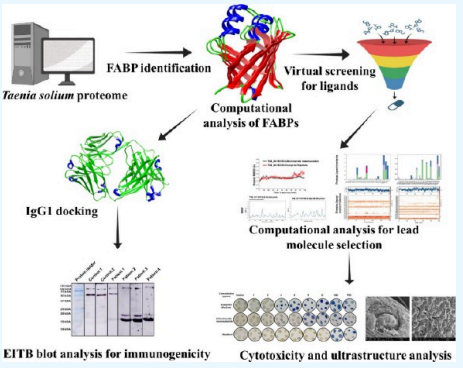

1. INTRODUCTION

Neurocysticercosis (NCC) is a formidable neuroinfectious condition due to the lodging of *Taenia solium* larvae into the human central nervous system. Its predominant clinical manifestation are recurrent seizure episodes or epilepsy. NCC is responsible for close to 29% of all acquired epilepsy cases worldwide.[1] Although this disease is prevalent across the globe, high incidences are reported from developing countries, and the World Health Organization (WHO) categorizes it as one of the Neglected Tropical Diseases (NTDs). It is predominant in economically underprivileged communities due to poor hygiene practices, drinking water contaminated with parasite eggs, and consumption of undercooked pork.[2] The causative parasite, *T. solium*, completes its life cycle between two hosts, i.e., pigs and humans. Pigs act as intermediate hosts harboring the parasite in cyst form, and humans act as definite hosts harboring both adult and cyst forms of infection. NCC is caused when humans consume contaminated water/vegetables having *T. solium* eggs. The egg hatches and develops into hexacanth embryo, which is efficient in breaching the blood−brain barrier (BBB) and can establish infection to any part of the body. But when it reaches the brain, it stays there for long time, evading the host immune system. However, a dying cyst loses this homeostasis and elicits an immune reaction that leads to seizure, and this is called NCC.[3]

Being an NTD, this disease also (like other NTDs) has several challenges related with its diagnosis, treatment, and understanding of its pathogenesis due to negligence from local governments as well as the scientific community. However, close to 1.5 billion people are anticipated to have helminthic infections worldwide, and hence, this parasite is in the list of WHO's target plan to eliminate top NTDs by 2030.[4] The major roadblocks to this target are the absence of reliable serodiagnostic tools, nonavailability of human vaccines, and unknown pathology of the disease.[5−7]

Eradication of the disease requires a thorough understanding of the parasite biology including the immune evasion strategy and alteration in cellular homeostasis of the host. It is well understood that like other parasites, *T. solium* is also deficient in essential constituents of the lipid biosynthesis cellular machinery and fulfill all its lipid requirement from the host with the help of Fatty Acid Binding Proteins (FABPs). FABPs ensure parasite mediated lipid uptake from the host for their

Received: November 20, 2023
Revised: April 22, 2024
Accepted: May 7, 2024
Published: May 15, 2024

https://doi.org/10.1021/acsomega.3c09253
ACS Omega 2024, 9, 22557−22572

growth and survival.[8,9] They are a cohort of low-molecular-weight proteins (with masses ranging from 13 to 15 kDa) characterized by a shared 10-stranded β-barrel architecture featuring a pair of elongated α-helices that interact with the ligands and facilitate lipid transport.[10]

Homology modeling provides the initial description of unknown proteins and have several advantages, such as it provides rapid identification and structure prediction, automation in the pipelines, and integration with large databases like PDB (Protein Data Bank), which are updated routinely. SWISS-MODEL is one of the modeling platforms that can provide putative structures along with the potential role of the protein.[11] Simultaneously, gene annotation platforms, like eggNOG-mapper, which is a computational platform, can provide functional annotation and ortholog assignment, can perform homology search, and may also perform phylogenetic analysis that helps to establish evolutionary relationships of genes. Acquiring knowledge about these parameters is essential for understanding biological processes and pathways.[12] In this study, we combined *in silico* screening with *in vitro* techniques to explore the involvement of FABPs in evoking the host immune response, understanding parasite survival mechanisms, and identifying potential drug targets and their application as potential diagnostic markers.

By using whole proteome scanning, we successfully identified five FABP proteins in the *T. solium* proteome. These FABPs were further analyzed for their structure, biological function, and immunogenicity (as potential vaccine and diagnostic antigens) and finally as a site for new drug targets.

2. MATERIALS AND METHODS

2.1. Protein Sorting for FABP Prediction. The annotated proteome of *T. solium* was sourced from the WormBase parasite database (https://parasite.wormbase.org/index.html). We then sorted the entire proteome based on their molecular weight and selected the proteins (1134 proteins in total) within the range of 12−16 kDa because the molecular weight range of FABPs is 13−15 kDa. The selected proteins were divided into two different molecular weight ranges, which were 12−14 and 14−16 kDa. These proteins were then used for homology modeling.

2.2. FABP Prediction Using SWISS-MODEL and Genome-wide Functional Annotation. The proteins that were sorted were employed for the purpose of homology modeling, employing the SWISS-MODEL online tool (https://swissmodel.expasy.org/) aimed at predicting FABPs within the proteomic composition of *T. solium*.[13,14] The FASTA files were used for protein prediction using SWISS-MODEL (https://swissmodel.expasy.org/interactive) that utilizes the Protein Data Bank (PDB) as reference database. Modeling was performed in automatic mode to select the most homologous template. We selected the proteins that have structural similarity with EgFABP1. Predicted models were then assessed for their identity percentage with the template protein, QEMAN score, and Ramachandran plot details. The secondary structure, relative conservation, and mutation-sensitive regions were predicted using the Phyre2 server (http://www.sbg.bio.ic.ac.uk/phyre2/index.cgi).[15] Genome-wide functional annotation in the KEGG pathway was analyzed using eggNOG-mapper (http://eggnog-mapper.embl.de/).[16] The molecular weights of identified proteins were predicted using the Expasy tool (https://web.expasy.org/compute_pi/).[17]

2.3. Multiple Sequence Alignment, Phylogenetic Tree Preparation, and Conserved and Mutational Sensitive Site Prediction. Following the FABP prediction from the comprehensive *T. solium* proteome, potential amino acid sequences corresponding to FABPs were retrieved from the WormBase parasite database ((https://parasite.wormbase.org/index.html) using sequence IDs.[18] These sequences were aligned using the MEGA software (https://www.megasoftware.net/),[19] and aligned input sequences were analyzed via the ClustalW module of the MEGA software using the Jones−Taylor−Thornton model. To construct a phylogenetic tree, the Maximum Likelihood Tree module was exercised by specifically utilizing the nearest-neighbor-interchange (NNI) inference algorithm. The discernment of conservation patterns and regions susceptible to mutations was undertaken through the utilization of the Phyre2 server intricately linked to an investigator module (http://www.sbg.bio.ic.ac.uk/phyre2/index.cgi).

2.4. Cysticercus Isolation and FABP RNA Expression Analysis. Cysticerci were taken from our earlier study.[20] Cysts were isolated from infected pig samples as described earlier.[21] The cyst viability was assessed by H&E staining on the tissue embedded cyst as described earlier.[22] RNA was purified from the isolated cysticerci using the Trizol method.[23] Subsequently, cDNA was prepared from extracted RNA employing the iScript Advanced cDNA Synthesis Kit (Bio-Rad, USA). The expressions of all FABPs were analyzed via sequence specific primers (Table S1).

2.5. Molecular Modeling, Cellular Localization, and Transmembrane-Helix and Phosphorylation-Sensitive Site Prediction. To obtain the tertiary structures of predicted proteins, the AlphaFold server was utilized.[24] Three-dimensional structures were rendered using the UCSF chimera software (https://www.cgl.ucsf.edu/chimera/).[25] The choice of the tool is contingent upon subsequent utilization for *in silico* docking investigations downstream. The GalaxyRefine server was leveraged for rigorous structural refinement of the built models, and structures were then assessed in the Ramachandran plot using the PROCHECK tool (https://servicesn.mbi.ucla.edu/PROCHECK).[26,27] Modeled structures were validated using the Prosa-Web server by calculating the *Z*-score that determines the errors in the structure (https://prosa.services.came.sbg.ac.at/prosa.php).[28] All of the models passed the quality analysis tools such as verify-3D and Errat (data not included). Cellular localization and transmembrane-helix predictions were done using the TMHMM (http://www.cbs.dtu.dk/services/TMHMM/) and Phobius software (https://phobius.sbc.su.se/).[29] Prediction of putative phosphorylation-sensitive amino acid residue positions was explored using the DEPP (Disorder Enhanced Phosphorylation Predictor) online server (http://www.pondr.com/cgi-bin/depp.cgi).[30]

2.6. Docking of Predicted Proteins against the IgG1 Fragment of the Antigen Binding (Fab) Region. Modeled structures of proteins were first prepared for docking using the AutoDockTools (ADT) graphical user interface (http://mgltools.scripps.edu/).[31] By exploiting the ADT interface, we eliminated heteroatoms and interface water molecules and incorporated Kollman charges and polar hydrogen atoms, and subsequent files were saved for further docking. The PDB structure of the IgG1 Fab region (PDB code: 3FZU) was

https://doi.org/10.1021/acsomega.3c09253
ACS Omega 2024, 9, 22557−22572

obtained from the RCSB PDB database and prepared for docking by using ADT through a similar approach. Prepared structures were docked using the HawkDock server (http://cadd.zju.edu.cn/hawkdock/).[32] HawkDock employs the ATTRACT algorithm for docking via the use of energy minimization that provides rotational degree of freedom to individual amino acids of protein and predicts desolvation energy of both the protein−protein interaction (PPI) complex and individual residues involved in protein−protein interaction. Docking starts with protein minimization for 100 steps with a distance squared cut value of 50 Å^2. Ten thousand decoy docked complex models were prepared post docking process, and 1000 best decoy models were selected by the ATTRACT algorithm and HawkRank module of the sever. Selected models were then clustered using the fraction of common contacts (FCC) method with an automated FCC threshold of 0.5, and the best selected models were rescored by the HawkRank module, providing results of the top 10 models and/or 100 models based on user application. For molecular mechanics/generalized born surface area (MM/GBSA) calculation, the *ff02* force field was applied. Missing hydrogen atoms and heavy atoms were added by the server in automated mode to the PPI complex via the *tleap* module of Amber16. Finally, the *ff02* force field was applied on the PPI complex, and optimization was done with 2000 cycles of steepest descent and 3000 cycles of conjugate minimizations. Dielectric constants of exterior and interior/solute were set to 80 and 1, respectively. The MM/GBSA value was then calculated by the modified GB (GB^{OBC1}) model on the HawkDock server.

2.7. Molecular Dynamics Simulation of Predicted FABPs-IgG1-Fab Complexes. Molecular dynamics (MD) simulation of the PPI complexes was performed using the Desmond module of Schrödinger, LLC (https://www.schrodinger.com/products/desmond).[33] Post-PPI complex uploading, bond order assigning in the preprocess option followed by water removal, hydrogen incorporation, and energy minimization in the refine section was performed using the protein preparation wizard. After protein preparation, the TIP3P water model system was selected in orthorhombic boundary conditions, and desired chloride ions with 0.15 M NaCl were selected as suitable buffer for MD simulation. The OPLS3e force field was employed in system building for MD simulation at the final stage. Finally, molecular dynamics of the complex was done at temperature and pressure of 310.15 K and 1.01325 bar, respectively, for the time period of 100 ns with capturing of each frame at 100 ps. The root mean square deviation (RMSD) of the C-α backbone and root mean square fluctuation (RMSF) of the relative PPI complexes were analyzed via the Origin 8.0 software.

2.8. Cloning, Expression, Purification, and Enzyme-linked Immunoelectrotransfer Blot (EITB) of TsM_001185100. Newly synthesized cDNA was utilized for cloning of TsM_001185100 using Phusion HF DNA polymerase (M0530S, New England Biolabs, UK) by sequence specific primers with restriction sites (Table S1). A gene was cloned in between Nde1(R0111S, NEB, UK) and XhoI (R0146S, NEB, UK) restriction sites in pET23a (V011017#, NovoPro, China) vector N-terminal of the 6-His-tag. Recombinant protein production was performed using induction with 1 mM IPTG (MB072-25G, HiMedia Laboratories, India) in C43 cells at 18 °C for 18 h. The lysed cell suspension was centrifuged at 21,000*g* for 20 min to separate supernatant and pellet fractions. The supernatant fraction was subjected to nickel-NTA chromatography (R90115, ThermoFisher, USA) through increasing concentrations of imidazole (I5513, Sigma-Aldrich, USA; 30, 100, and 250 mM) and visualized using SDS-PAGE gel electrophoresis. Pure fractions were then pooled and dialyzed against 1× potassium phosphate buffer (50 mM K_2HPO_4 and 50 mM KH_2PO_4) thrice at 4 °C on a magnetic stirrer. All the dialyzed protein was then concentrated using 10 kDa MWCO protein concentrators (88527, ThermoFisher Scientific, USA), filtered using 0.22 μM PES syringe filters (09-740-113, ThermoFisher Scientific, USA), aliquoted, and stored at 80 °C for future use.

NCC positive and negative serum samples were used from a previously approved study, and EITB (enzyme-linked immunoelectrotransfer blot) was performed as described earlier.[34] In a concise manner, 10 μg of freshly purified TsM_001185100 was subjected to 12% SDS-PAGE followed by transfer onto a PVDF membrane. The membrane was subsequently sectioned into distinct strips and allowed an overnight incubation at 4 °C with serum (diluted 1:200 in 5% BSA in 1× TBST) obtained from both NCC-negative and NCC-positive patients. Next day, the membrane underwent three 5 min washes with 1× TBST and was then incubated with a 2° antihuman antibody (I2136, Sigma-Aldrich, USA). Immunoblots were developed on an Amersham Imager 600 series (GE Healthcare, USA).

2.9. Ligand Binding Residue Prediction and Drug Screening. Modeled structures of potential TsMFABPs were then analyzed for ligand or fatty acid interacting residues. For model examples, four different neutral lipids—arachidonic acid, linoleic acid, oleic acid, and palmitic acid—were used for the study. Reference structures of respective ligands were obtained from the PubChem database (https://pubchem.ncbi.nlm.nih.gov/).[35] A grid was prepared around a previously identified druggable site, and ligands were docked into the site using the GLIDE module to get the most stable conformations with respective binding energies and ligand interacting residues. Conformations of relative docked structures were captured using the ligand interaction diagram module. Post ligand interactive residue prediction, DrugBank approved and investigational drug library was docked in the druggable site, and compounds with the most negative binding energies were selected for investigational studies. The top compounds were selected, the conformational duplicates were removed, and then these compounds were further screened with the Lipinski rule of five to get pharmacologically suitable candidates.[13] Molecular dynamics simulation was performed using a Schrodinger software suite. RMSD values were calculated using the Schrödinger "Molecular dynamics" package and plotted using the OriginPro 8.0 tool. RMSF values and amino acid hotspot plot were generated using Schrödinger. After filtering, selected ligands that have the capacity of the penetrating blood−brain barrier were searched in the literature. Selected compounds were then used for *in vitro* cysticidal assays.

2.10. *In Vitro* Cysticidal Activities. *T. solium* cysticerci were seeded in six-well plates (five cysts/well) and then incubated with increasing doses (1, 2, 4, 8, 16, and 32 μg/mL) of enalaprilat dihydrate (resuspended in dimethyl sulfoxide (DMSO), E9658, Sigma-Aldrich, USA, ≥98% purity), β-nicotinamide mononucleotide (resuspended in 1× PBS, N3501, Sigma-Aldrich, USA, ≥95% purity), and riboflavin (resuspended in 1× PBS, R9504, Sigma-Aldrich, USA, ≥98% purity) for 48 h alongside the experimental control in 37 °C

https://doi.org/10.1021/acsomega.3c09253
ACS Omega 2024, 9, 22557−22572

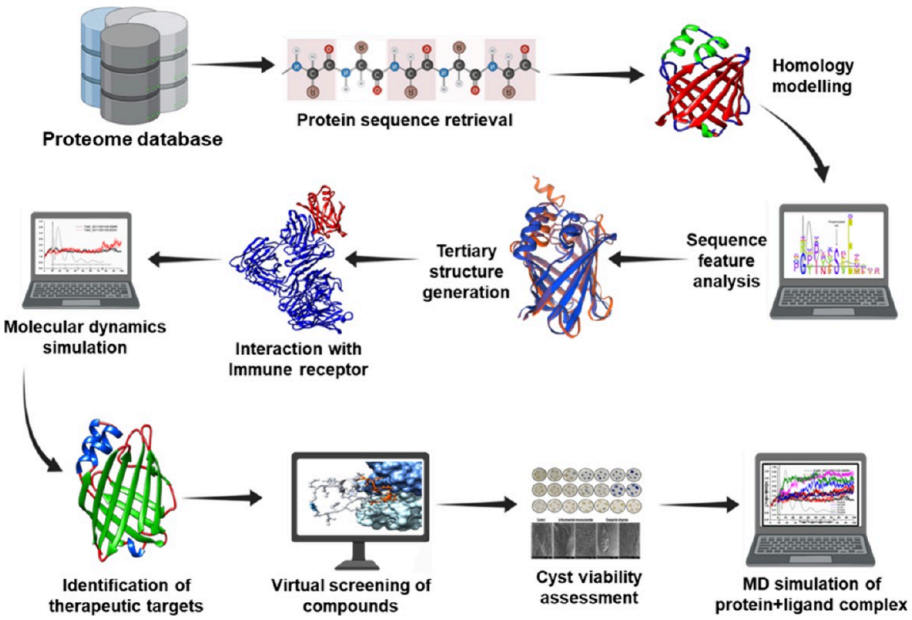

Figure 1. Pipeline for predicting the *Taenia solium* fatty acid binding protein superfamily and analysis of immunological property and use as potential therapeutic targets.

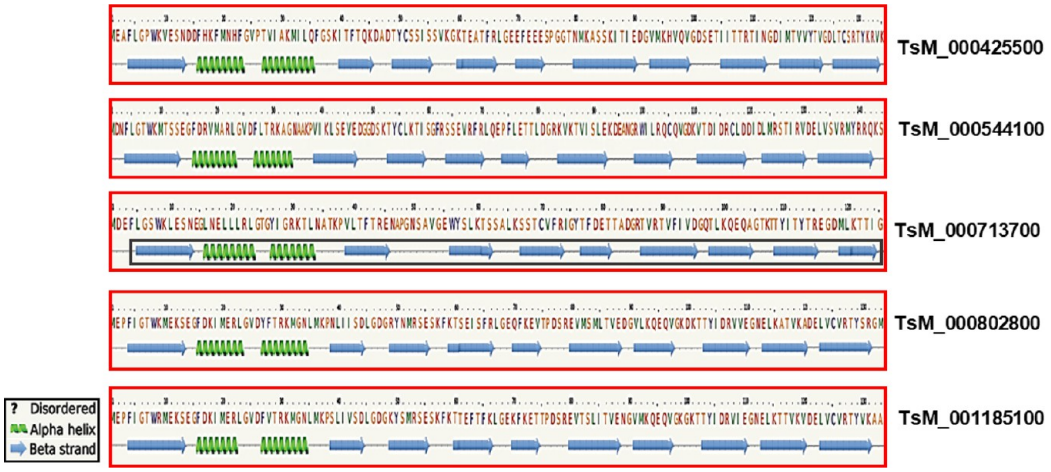

Figure 2. *T. solium* expresses five fatty acid binding proteins in its proteome. The secondary structure of the proteins was predicted using the Phyre2 server where all proteins have 2 α-helices and 10 β-sheets (except TsM_000713700 that has 9 β-sheets). For secondary structure prediction, a query on the hidden Markov model was applied, i.e., looking for similar structure in the existing database.

humidified 5% CO_2 incubator (Eppendorf, Germany). DMSO was used as negative control for enalaprilat dihydrate. Post 48 h of incubation, culture media were aspirated, and the cysticerci were subjected to two consecutive washes with 1× phosphate buffer saline (PBS). Following this, they were immersed in 1× trypan blue dye for a duration of 30 min within a humidified incubator maintained at 37 °C and 5% CO_2. Post incubation, cysticerci were extensively washed with 1× PBS to remove the unbound dye, and cysticidal activity was determined by visualizing the dye uptake by the cysticerci.

2.11. Scanning Electron Micrographs (SEMs) of Cysticerci. Drug-treated cysticerci were then used for SEM as described.[36] In brief, all the cysticerci were fixed using 3% formaldehyde prepared in 1× PBS for 10 min at RT. Subsequently, the cysticerci were washed twice with 1× PBS and then serially dehydrated using gradients of ethanol (50, 70, 90, and 95%) in water for 2 min each. Post dehydration, cysticerci were coated with 5 nm of gold for conductivity, and SEM images were captured for analyzing the altered changes in the surface morphology compared to control.

3. RESULTS

3.1. Exploring the *T. solium* Fatty Acid Binding Protein (FABP) Family and KEGG pathway Annotation. Based on molecular weight criteria for predicting FABPs, we identified a total of five FABPs in the *T. solium* proteome. The pipeline used to identify FABPs was based on homology modeling based approach and downstream analysis workflow (Figure 1).

The molecular weight varied from 13 to 15 kDa. These FABPs are TsM_000425500 (135 aa), TsM_000544100 (144 aa), TsM_000713700 (125 aa), TsM_000802800 (133 aa), and TsM_001185100 (133 aa). All the predicted TsMFABPs shared common homology with the *Echinococcus granulosus* fatty acid binding protein 1 (EgFABP1) and were named accordingly by following the convention (Table S2).

https://doi.org/10.1021/acsomega.3c09253
ACS Omega 2024, 9, 22557−22572

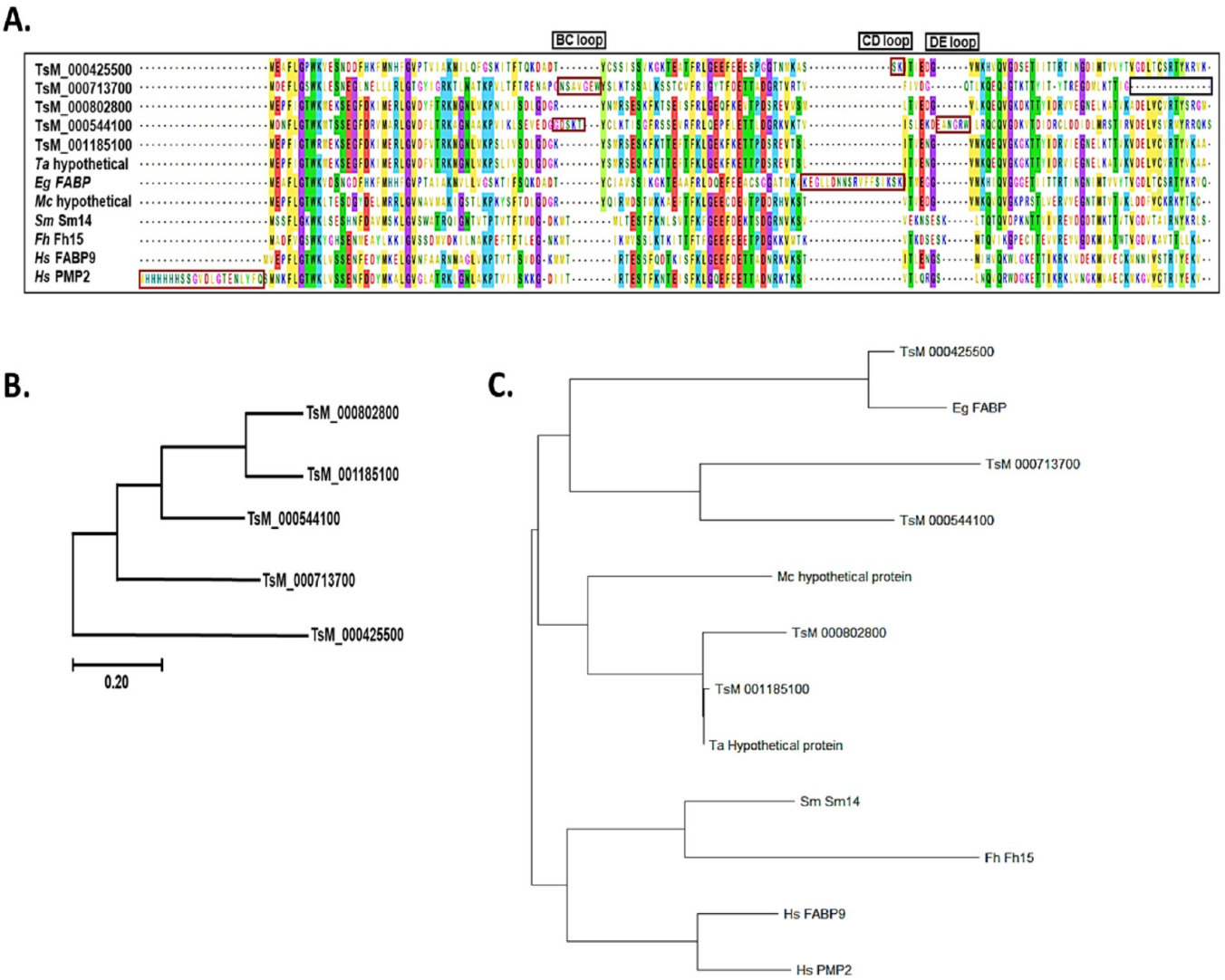

Figure 3. All five predicted proteins were compared with FABP proteins from other species including *H. sapiens*. (A) Multiple sequence alignment was performed using the clustalW module of the MEGA software. Amino acid extensions are indicated in red boxes, whereas the C-terminal gap in TsM_000713700 is indicated with a black box. (B) Maximum likelihood phylogenetic tree analysis of all predicted proteins was constructed using the MEGA software (version 10). The maximum likelihood tree was constructed for all five *T. solium* FABPs (C) and all five *T. solium* FABPS, *E. granulosus* FABP, *M. corti* hypothetical protein, *T. asiatica* hypothetical protein, *S. mansoni* Sm14, *F. hepatica* Fh15 protein, *H. sapiens* FABP9, and *H. sapiens* PMP2 protein. The Jones−Taylor−Thornton (JTT) model was used with the nearest-neighbor-interchange (NNI) as the tree inference method to construct the phylogenetic tree.

Among the five proteins, four proteins have 2 α-helices and 10 β-sheets in their secondary structure. However, TsM_000713700 has only 9 β-sheets, and all the other amino acids form loops and α-helices in their secondary structure (Figure 2).

Combining the features of their secondary structures, they form a common 10-stranded β-barrel (except TsM_000713700 that forms a 9-stranded β-barrel structure) and 2 α-helices as potential regulatory element for lipid capturing. TsM_001185100 and TsM_000544100 were previously reported as TsMFABP1 and TsMFABP2, in which TsM_001185100 is secreted extracellularly and TsM_000544100 is found to be restricted to the cytoplasm. Individual proteins were then mapped for their KEGG pathway involvement, and we identified that TSM_000425500, TsM_000544100, TsM_000802800, and TsM_001185100 are involved in PPAR-γ signaling pathway (Figure S1A,B,D,E). Both TsM_000713700 and TsM_001185100 are involved in regulation of lipolysis; however, TsM_000713700 is not predicted to be involved in the PPAR-γ pathway (Figure S1C,E). In conclusion, the KEGG pathway suggested that the function of predicted FABPs is predominantly restricted to PPAR-γ signaling and regulation of lipolysis in *T. solium*. PPAR-γ signaling is critical for regulating the pathways involved in inflammation, metabolism, and adipogenesis and responds to lipid mediators.[37] FABP mediated lipid transport from the host to helminth parasites is well established; thus, *T. solium* FABPs facilitate lipid uptake and mediate PPAR-γ signaling. Additionally, PPAR-γ also upregulates the catalase and superoxide dismutase expression, suggesting that the parasite may utilize the PPAR-γ enzyme for suppressing the oxidative stress.[38] PPAR-γ also plays a significant role in the regulation of lipolysis, and in our analysis, FABPs were also predicted to have a role in the regulation of lipolysis in the parasite.[39] Helminth parasites have lipid modification enzymes, and *T. solium* FABPs might have

https://doi.org/10.1021/acsomega.3c09253
ACS Omega 2024, 9, 22557−22572

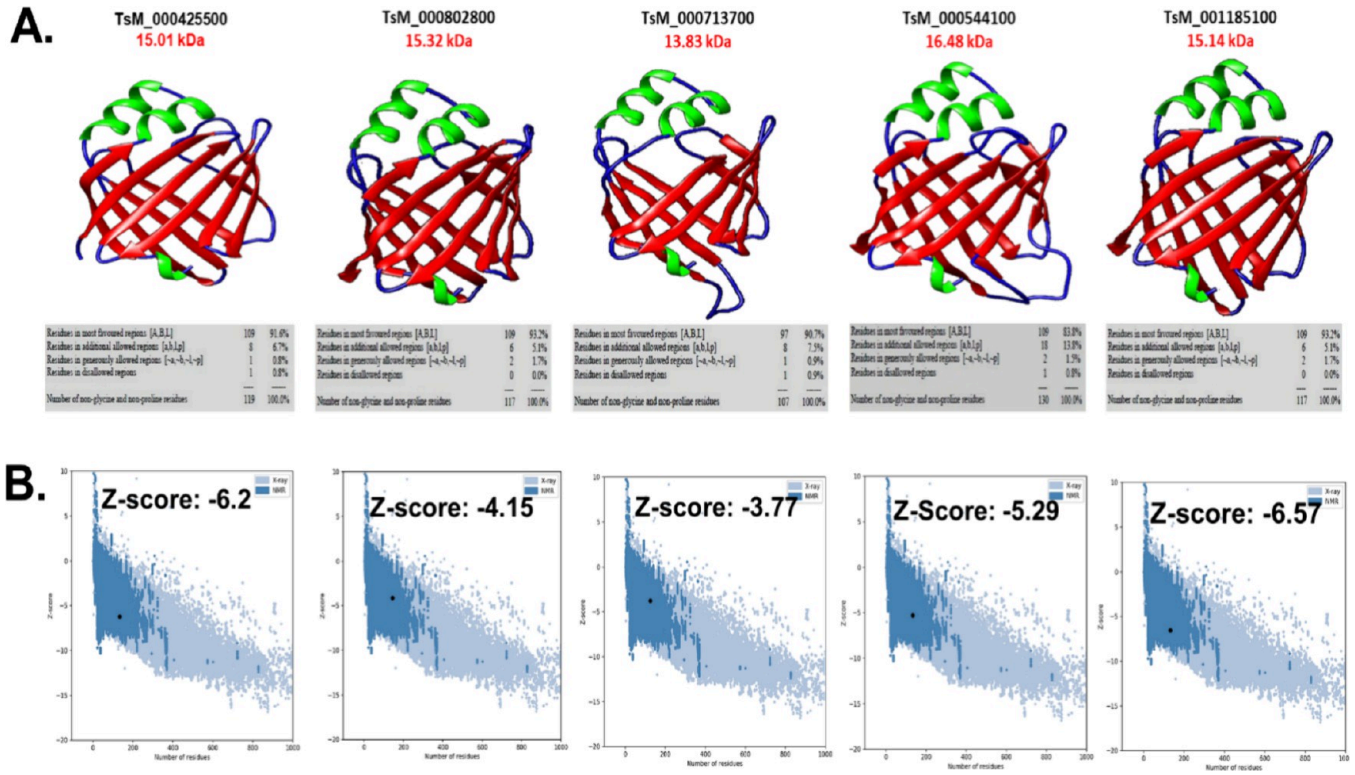

Figure 4. Molecular modeling was done using AlphaFold in automated mode. (A) All modeled structures were visualized using the UCSF chimera software, and secondary structures were represented using different colors (green: α-helix, red: β-sheets, blue: loop region) along with their Ramachandran plot allowed percentages. As shown in the figure, all five predicted TsMFABPs have a common β-barrel-like structure with two extended α-helices. (B) Structural error analysis (negative value indicates stable structures) of respective proteins.

some role in either lipid breakdown or lipid modification processes, but the exact function is still unclear.[40]

3.2. Multiple Sequence Alignment and Phylogenetic Analysis. Multiple sequence alignment of all predicted TsMFABPs showed that TsM_000713700 and TsM_000544100 have an extended stretch of amino acid residues in the BC loop, TsM_000544100 has an additional amino acid stretch in the DE loop, whereas TsM_000425500 has two additional amino acids in the CD loop (Figure 3A). However, the biological or functional significance of the extended amino acid regions has yet to be investigated. As described earlier, TsM_000713700 lacked amino acid stretch in the C-terminal, which could be responsible for nine β-sheets in the β-barrel structure.

Multiple sequence alignments of all five predicted proteins revealed that TsM_000425500 evolved distantly from the other four proteins (Figure 3B). Sequence alignment with other species indicates that TsM_000425500 is related to EgFABP and that TsM_000713700 and TsM_000544100 are related to each other, whereas TsM_000802800 and TsM_001185100 are closely related to *T. asiatica* (Figure 3C). Lipids usually bind to the β-barrel like cavity on FABPs and are subsequently transported across the cell membrane. Certain amino acids in the β-barrel cavity interact with the ligands and facilitate the transport. The amino acid residues that are not involved in the functional role are subjected to mutational sensitivity and are less prone to conservation. We also noticed relative conservation in all five putative TsMFABPs and observed that amino acid residues that are less susceptible to conservation are mostly associated with the β-barrel and one of the α-helices (Figure S2A). However, no reports are available regarding the amino acid modifications in the individual TsMFABPs in *T. solium*. Mutation sensitive regions were also analyzed in the primary amino acid sequences of predicted proteins. We observed moderate to low mutation sensitive regions in the protein sequences (Figure S2B). Few residues in the β-barrel structures have been found to be more sensitive to mutation, which need to be explored further for their biological significance associated with the survival of *Taenia* parasite.

3.3. Molecular Modeling, Cellular Localization Prediction, and Putative Phosphorylation Site Prediction. All FABPs in helminth parasites share a common 10-stranded β-sheet conformation with two extended α-helical regions joined by loop forming residues. Molecular modeling of all predicted proteins revealed their β-barrel structure. The three-dimensional structure of these proteins followed the same pattern as that of their predicted secondary structure. TsM_000713700 has 9 β-sheets in the β-barrel structure, whereas the other four proteins (TsM_000544100, TsM_000713700, TsM_000802800, and TsM_001185100) have characteristic 10 β-sheets in the β-barrel structure (Figure 4).

Each modeled structure was then tested for 3-D structure. A negative *Z*-score value for all the proteins was observed, which indicated negligible errors while modeling and the integrity of modeled structures present at the native conformations (Figure 4). A previous report has shown the secretory behavior of TsM_001185100 (TsMFABP1) and its enrichment in the ESPs.[41] We analyzed the localization and transmembrane region prediction of all the proteins and found that TsM_000425500 protein has some residues (20th−36th

https://doi.org/10.1021/acsomega.3c09253
ACS Omega 2024, 9, 22557−22572

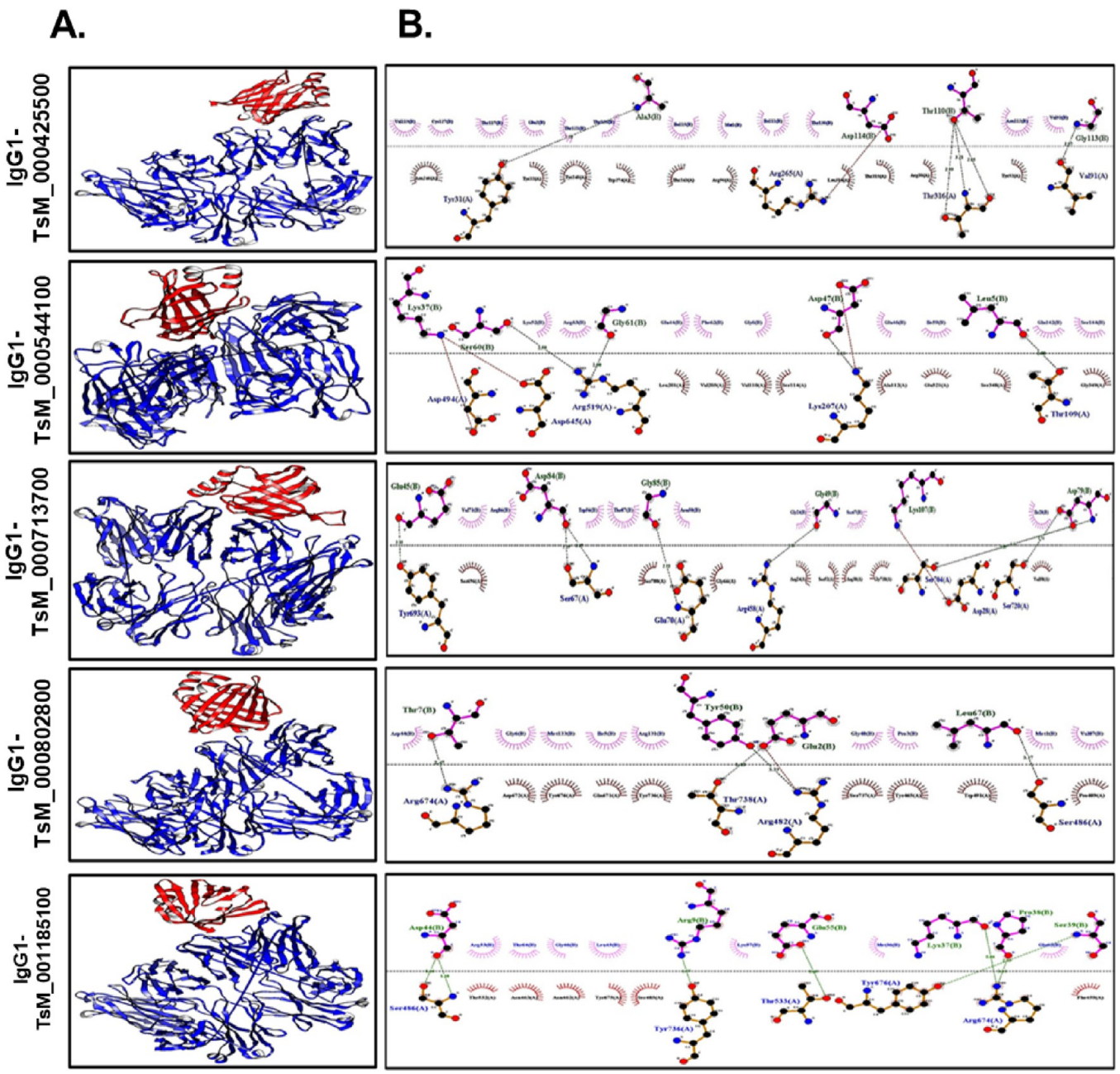

Figure 5. Docking study was performed of modeled FABPs with the immunoglobulin IgG1 Fab region (3FZU: PDB ID) using the HawkDock server. (A) FABPs were docked on IgG1 Fab regions using the HawkDock server. (B) Docked complexes are shown in the figure with their respective hydrogen bonding status and amino acid residues involved in hydrogen bonding using the LigPlot software.

position amino acid stretch) that are capable of binding to the membrane and can be secreted in the extracellular environment by the *T. solium* parasite (Figure S3A,B, Table S3). We did not find any secretory feature in the TsM_001185100, which suggests that it might be secreted outside by *T. solium* via some unconventional route. The other FABPs—TsM_000544100 (TsMFABP2), TsM_000713700, and TsM_000802800—were restricted to cytosol for their localization.

Post-translational modification plays a critical role in the function of many proteins. It can either activate or deactivate protein function. Previously, phosphorylation was associated with the regulation of FABP3 protein function in *Homo sapiens*.[42] We also analyzed the putative amino acid residues that are sensitive to phosphorylation. We found that serine and threonine are putatively involved in the phosphorylation of most of these proteins. Serine phosphorylation was not observed in TsM_000713700, whereas tyrosine phosphorylation was predicted in TsM_001185100 (Figure S4, Table S4).

3.4. Molecular Dynamics Simulation of Predicted Protein, IgG1-Docked Protein Complexes, and Immunoreactivity Analyses by EITB. The modeled proteins were analyzed for their stability, and it was found through MD simulation that TsM_000544100 and TsM_001185100 have maximum stability compared to the other three proteins (Figure S5). The TsM_000713700 has maximum deviation in

https://doi.org/10.1021/acsomega.3c09253
ACS Omega 2024, 9, 22557−22572

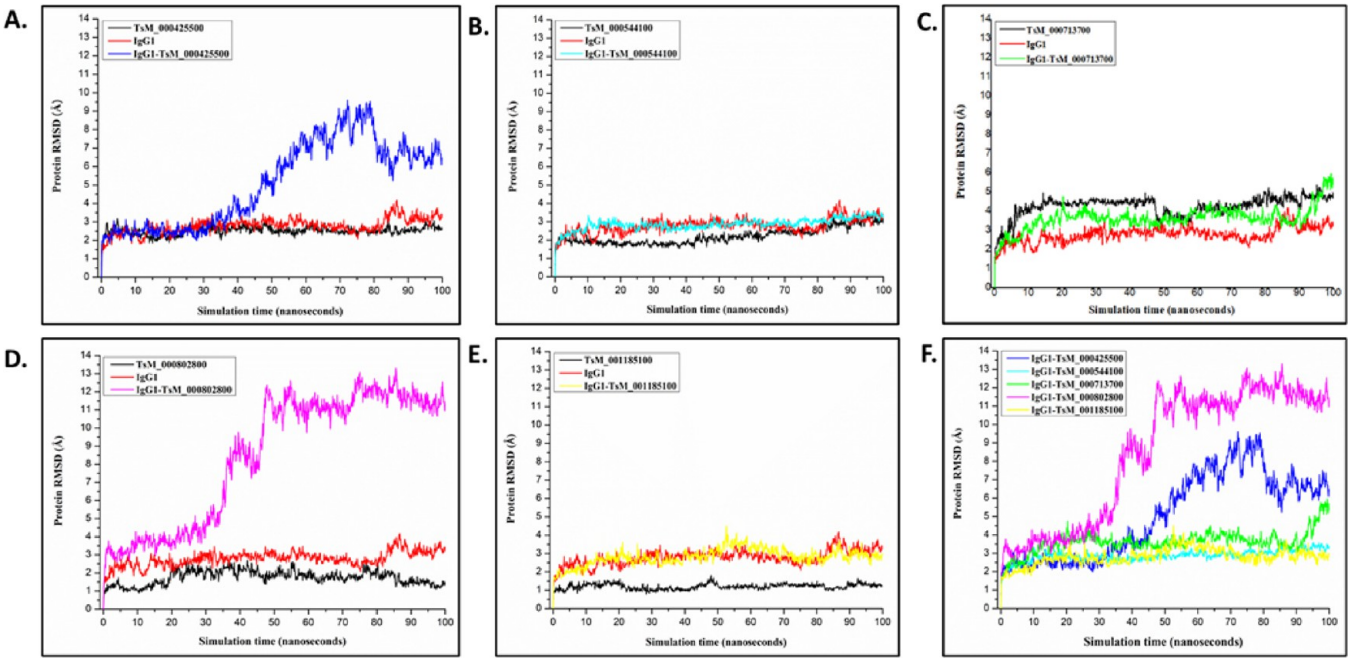

Figure 6. TsMFABPs (TsM_000544100 and TsM_001185100) showed stability with the IgG1-Fab region and was highly immunoreactive to NCC positive patient serum samples. The stability of predicted proteins complexed with the IgG1 Fab region was analyzed using molecular dynamics simulation. (A–E) These figures show the comparative MD simulation trajectories of all five predicted proteins, all five proteins complexed with IgG1 immunoglobulin, and IgG1 alone over the time period of 100 ns (0.15 M NaCl solution as the buffer system). (F) The cumulative stability plots of all complexes for comparative analysis. RMSD data were plotted using the Origin 9.0 software.

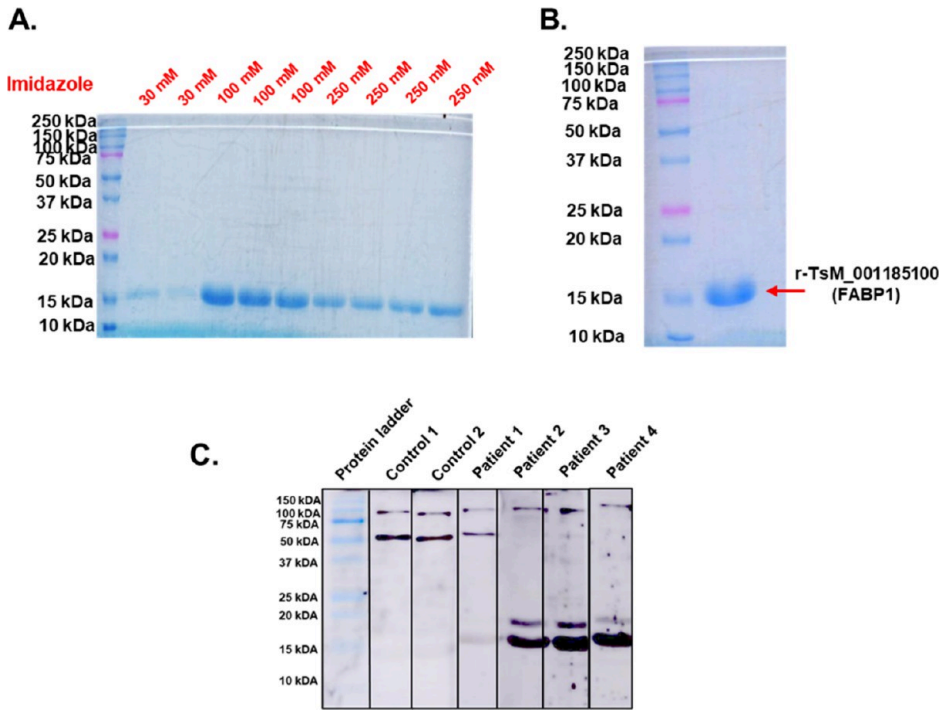

Figure 7. Recombinant TsM_001185100 (TsFABP1) showed immunoreactivity against NCC positive serum samples. r-TsM_001185100 was purified using Ni-NTA affinity chromatography. (A). SDS-PAGE and Coomassie brilliant blue (CBB) stained image of different fractions purified using increasing concentrations of imidazole. (B). Purified r-TsM_001185100 is an approximately 16 kDa protein in CBB stained SDS-PAGE gel electrophoresis. (C). EITB blot of r-TsM_001185100 showed that the protein is highly cross-reactive against NCC positive patients' serum samples.

the total simulation time frame, whereas TsM_000425500 and TsM_000802800 show moderate stability.

Helminth FABPs are known to be antigenic in nature and have potential to be used in the diagnosis of infection. Additionally, they serve as potential vaccine candidates.[10,43] The IgG1 antibody response strongly correlates with soluble and membrane protein antigens.[44] Hence, each protein was then analyzed for their putative antibody responses and T-

https://doi.org/10.1021/acsomega.3c09253
ACS Omega 2024, 9, 22557−22572

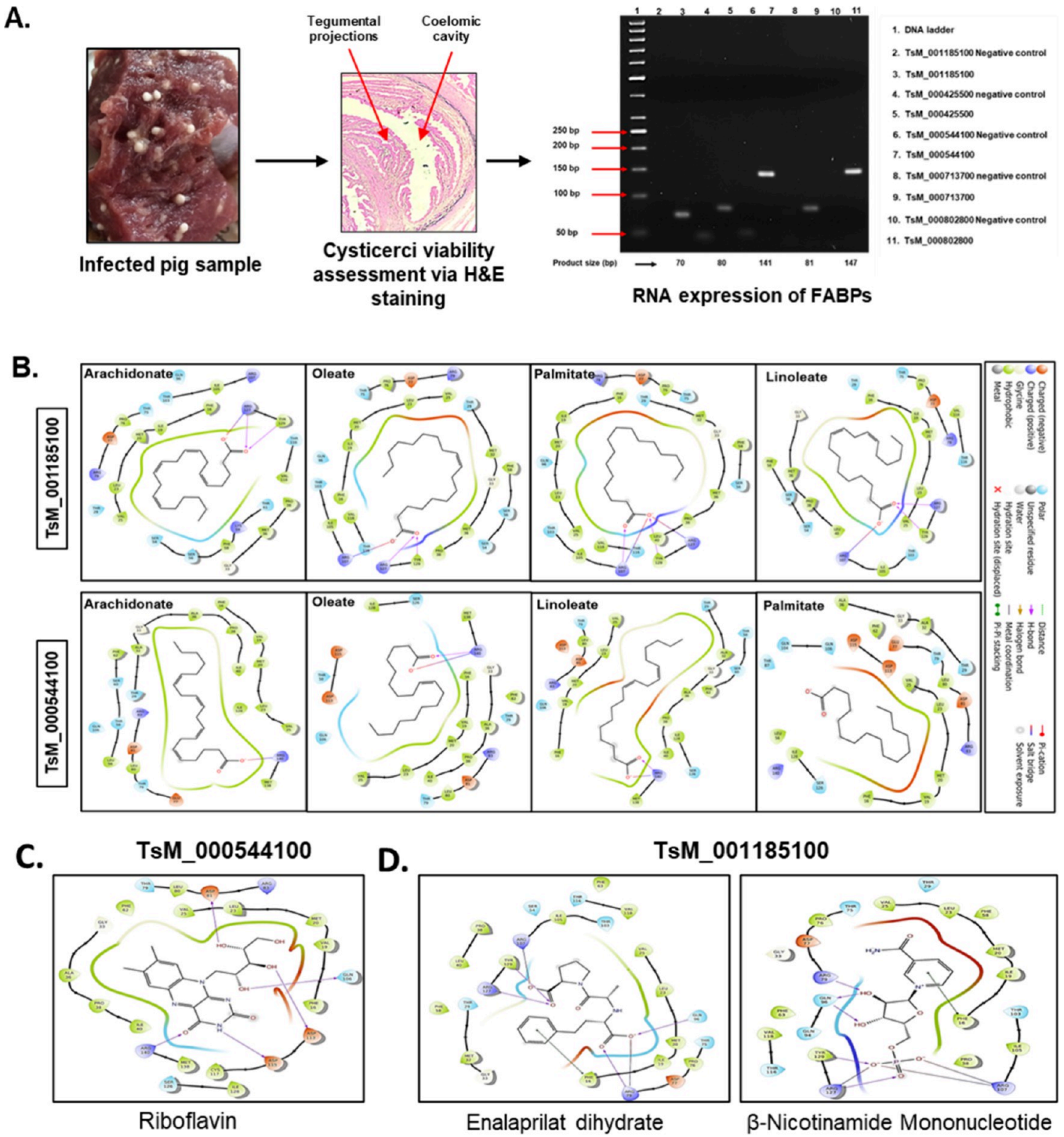

Figure 8. FABP expression at the RNA stage and investigation as therapeutic targets (A). Cyst isolation, RNA extraction, and agarose gel electrophoresis image showing the expression of each TsMFABP after PCR of respective cDNA from the total RNA of *T. solium* RNA. The druggable site was predicted using the sitemap module of the Schrödinger software. Post druggable site prediction, four known fatty acid ligands were docked to identify ligand binding residues. Docking of ligands into the predicted site was done using the Maestro Glide module. (B) As seen in the snapshot images, Arg107, Arg127, and Tyr129 of TsM_001185100 form interaction with the ligands, and Arg140 of TsM_000544100 forms interaction with the ligands. We did not see any ligand binding residue of TsM_000544100 forming interaction with the palmitate. The druggable site was predicted using the sitemap module of the Schrödinger software. DrugBank-approved and investigational drug library was screened against the druggable site using the Glide module, and resultant drugs were then searched in the literature for their blood−brain barrier penetration abilities. (C). Interaction diagram of riboflavin against TsM_000544100. (D) Interaction diagram of enalaprilat and *β*-nicotinamide mononucleotide against the TsM_001185100.

helper and memory cell proliferation prediction. Upon analysis, we identified that TsM_000425500 had the highest IgG (IgG1 + IgG2) antibody titer with the highest levels on the 50th day followed by steady-state levels at >25,000 until the 350th day postinjection followed by TsM_001185100, which follows the same trend as TsM_000425500 with steady-state titer of

https://doi.org/10.1021/acsomega.3c09253
ACS Omega 2024, 9, 22557−22572

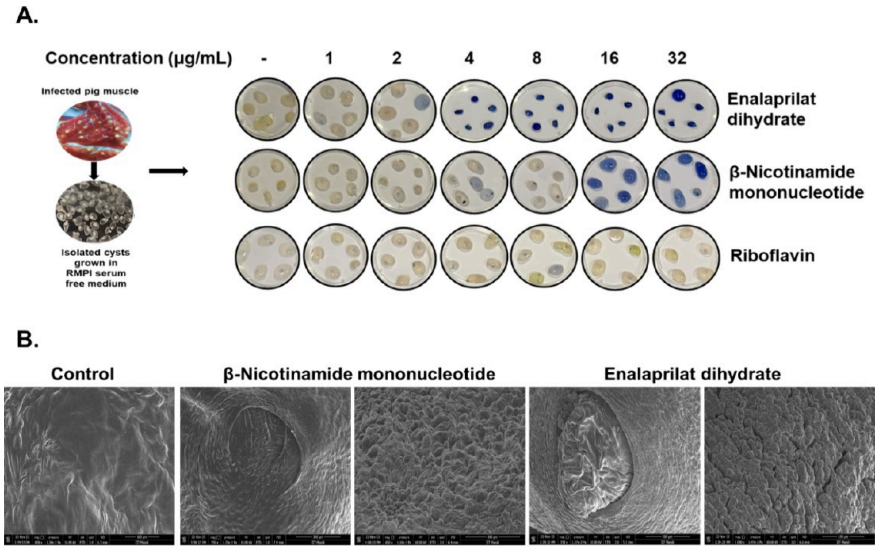

Figure 9. FABP effectively serves as a potential therapeutic target. (A). Cyst viability was decreased with enalaprilat dihydrate (4 μg/mL) and β-nicotinamide mononucleotide (16 μg/mL) but not with riboflavin. (B). Scanning electron microscopy revealed the altered surface morphology of the cyst wall after incubation with compounds as indicated.

>10,000 au from the 150th day to 350th day postinjection (Figure S6A). With regard to the T-helper memory cell proliferation, a similar trend was observed with all the proteins (Figure S6B). The modeled structures were further docked onto the IgG1-Fab1 region using the HawkDock server (Figure 5). Post docking, binding energies of the complexes were calculated using the MM/GBSA prediction platform of the HawkDock server, and it was predicted that the TsM_000425500-IgG1 complex has the maximum binding energy of −63.12 kcal/mol followed by the TsM_000802800-IgG1 complex with the maximum binding energy of −58.48 kcal/mol (Table S5).

Binding energies of the other three protein−protein complexes also showed stable complexes as TsM_000544100-IgG1, TsM_000713700-IgG1, and TsM_001185100-IgG1 had binding energies of −8.29, −29.49, and −33.14 kcal/mol, respectively. Docked complexes were then analyzed for their stability by RMSD calculation of backbone C-α carbon deviation from the original structure, which revealed that TsM_000544100-IgG1 and TsM_001185100-IgG1 form the most stable complexes with the least deviation (Figure 6A−F).

TsM_000713700 also formed a stable complex with the IgG1 Fab region, but its stability was disrupted after 80 ns (Figure 6C). Besides having the highest binding energies among all complexes, TsM_000425500 and TsM_000802800 form the least stable complexes with the IgG1 Fab region (Figure 6A,D). Consequently, MD indicated the possible role of TsM_000544100 and TsM_001185100 in activating the humoral immune response in the host system post *Taenia* infection. Previously, NCC positive patients' serum samples were demonstrated as positive against anti-IgG antibodies.[45] The humoral immune response in parenchymal NCC has been associated with IgG1, IgG2, and IgG4, whereas extraparenchymal NCC has been linked with IgG responses in CSF samples.[46] In another study, recombinant rFhFABP-V from *Fasciola hepatica* showed cross-reactivity against IgG antisera compared to IgM antisera, showing the antigenic nature of FABP proteins.[47] Secretory proteins are critically important in different infectious diseases as they directly interact with the immune system, help in establishing the infection, and can promote the inflammation. TsM_001185100 is one of the key proteins that has previously been reported to be detected in both cysticerci and outside in the host tissue.[41] To validate our findings in MD simulation, we purified TsM_001185100 (TsFABP1), which is secretory in nature, and performed EITB that showed strong immunoreactivity against NCC serum samples near 16 kDa that was not observed in NCC negative serum samples (Figure 7A−C). In one of the NCC positive patient's serum samples, r-TsM_001185100 showed less cross-reactivity compared to others; however, a greater number of serum samples are required to test the efficacy of TsM_001185100 as a potential vaccine candidate.

3.5. All FABPs Showed Expression at the RNA Level and Were Investigated as Potential Therapeutic Targets. FABPs play a very critical role in lipid transport into the extracellular and intracellular regions of a cell. Ligand interacting residues play an important role in lipid binding and establishing a stable interaction with the ligands. We validated the expression of all proteins at the RNA level (Figure 8A). The presence of TsMFABPs was confirmed by RT-PCR using primers designed against coding sequences (CDS) (Table S1). Only TsM_001185100 and TsM_000544100 have been reported to be expressed at the protein level, which suggest that there is a need to further explore this by using advanced proteomics tools.

Then we tried to identify the binding site of these FABPs with a few common lipids with a broader idea of identifying the druggable site for putative drugs. We identified the ligand binding site of these FABPs, docked four different ligands (palmitate, oleate, arachidonate, and stearate), and deduced that Arg107, Arg127, and Tyr129 of TsM_001185100 and Arg140 of TsM_000544100 are interacting (salt bridge and hydrogen bonding) with the ligands (Figure 8B).

There was no interaction between any amino acid residue in the TsM_001185100 protein and palmitate as the ligand. Ligand interacting residues play a critical role in ligand binding and thus can be a suitable target for compounds that can inhibit TsM_0005441100 and TSM_001185100 function. Post druggable site identification, we docked the DrugBank-

https://doi.org/10.1021/acsomega.3c09253
ACS Omega 2024, 9, 22557−22572

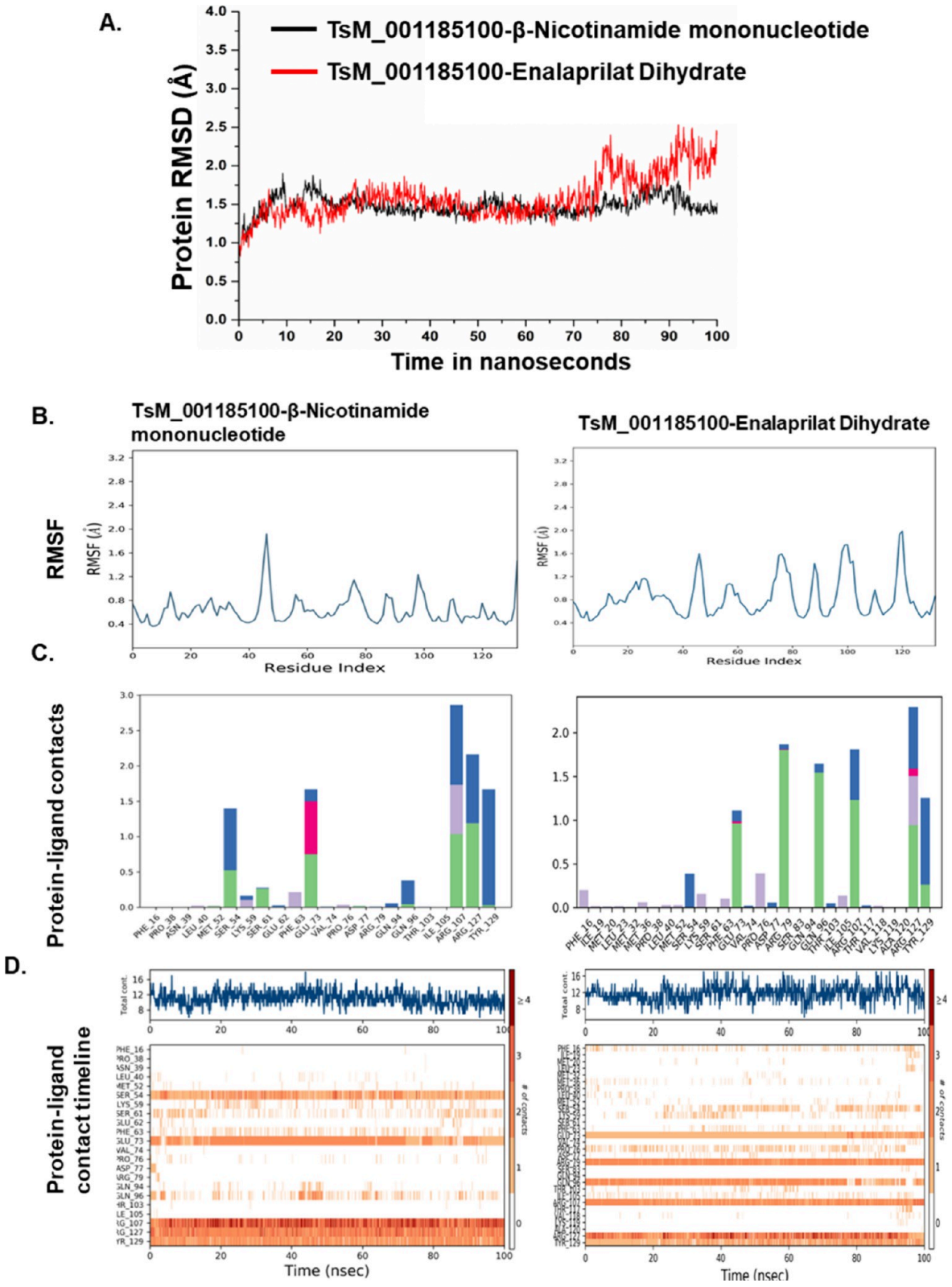

Figure 10. MD simulation analysis suggests the stable interaction between TsM_001185100 and enalaprilat dihydrate and *β*-nicotinamide mononucleotide where the compounds are predominantly interacting in the *β*-barrel region. (A) RMSD plot of protein ligand complexes for 100 ns time period. (B) RMSF plot showing minor fluctuations in amino acids of proteins during simulation. (C) Colored histogram plot of multiple interactions formed by amino acid residues of FABPs with selected ligands. (D) The 100 ns contact-based timeline depiction of entire contacts made by TsMFABPs with selected compounds. In the MD (molecular dynamics) simulation study, both the ligands, *β*-nicotinamide mononucleotide and enalaprilat dihydrate, showed stable interaction with the TsM_001185100 protein for 100 ns time, and Arg107, Arg129, Tyr129, and Glu73 were the predominant ligand interacting residues for the entire time frame of simulation (A–D).

https://doi.org/10.1021/acsomega.3c09253
ACS Omega 2024, 9, 22557−22572

approved drug library and selected compounds based on their interaction with the ligand interacting residues to identify new drugs against NCC. The top compounds were selected, and duplicates were removed and screened for completing the Lipinski rule of five criteria. Post screening, the compounds that can cross the blood−brain barrier were selected (as this infection persists in the central nervous system), and we identified that riboflavin can be used to target TsM_000544100 function (Figure 8C). Enalaprilat dihydrate and β-nicotinamide mononucleotide can be used to target the function of TsM_001185100 (Figure 8D). Considering the dominant role and function of FABPs in the growth of parasites, we explored them as potential therapeutic targets to assess cyst viability.

Enalaprilat Dihydrate Showed Effective Cysticidal Activity *In Vitro*. TsM_001185100 and TsM_000544100 were found to be suitable for drug targeting as both were found to have stable structures during MD simulation analysis and were reported to be expressed at the protein level in the cysticercus stage. Enalaprilat dihydrate (−30.1 kcal/mol) and β-nicotinamide mononucleotide (−40.73 kcal/mol) were identified against TsM_001185100 as potential inhibitory molecules. In case of TsM_000544100, riboflavin (−52.9 kcal/mol) was identified to be inhibitory, but no cysticidal activity was observed (Figure 9A). Enalaprilat dihydrate was identified as the best lead compound with the cysticidal activity at the lowest concentration (4 μg/mL), whereas β-nicotinamide mononucleotide showed cysticidal activity at 16 μg/mL (Figure 9A).

The determination of the surface morphology of cysticerci treated with enalaprilat dihydrate and β-nicotinamide mononucleotide showed disruption on the cyst surface compared to the untreated cysticerci (Figure 9B), which signifies the death of the cyst.

3.6. MD Simulation Revealed Stable Interaction in the Ligand Protein Complex. Enalaprilat dihydrate and β-nicotinamide mononucleotide were further investigated to determine whether they form a stable interaction with the ligands. We performed 100 ns time-scale MD simulation of ligand protein complexes that revealed a stable interaction between TsM_001185100 and ligands. In the RMSD plots, both the ligands showed stable binding for 100 ns; however, enalaprilat dihydrate showed a slight fluctuation up to 3 Å (Figure 10A).

In the RMSF plots, the fluctuations were also limited up to 2 Å, supporting the stable binding between protein and ligands (Figure 10B). In the case of β-nicotinamide mononucleotide, Arg107, Arg129, Tyr129, and Glu73 from TsM_001185100 are the predominantly interacting residues for the 100 ns MD simulation time, whereas on the other side with enalaprilat dihydrate, Arg127, Tyr129, Arg107 Gln96, Arg79, and Glu73 are the major residues from TsM_001185100 (Figure 10C). Overall, Arg107, Arg129, Tyr129, and Glu73 are the major ligand interacting residues for both the proteins (Figure 10D).

4. DISCUSSION

Homology-based prediction methods provide the easiest way to predict possible protein structure and function.[11,48] Predicted structures can be validated using different open access tools to determine authenticity and therefore can be used for different studies.[6,27,28] Protein modeling follows the principle of homology modeling and model protein structures using the BLASTP algorithm and uses solved protein structure as a template protein, thus providing authentic 3-D structures of the proteins.[49] Solving protein structure via experimental methods like cryo-EM and X-ray crystallography is time-consuming and cost intensive; thus, computational homology-based methods serve as more reliable tools to provide an initial idea about possible protein structures.[50] FABPs are present in many isoforms across eukaryotes, working in different locations in the cell (cytosol, organelle, and extracellular regions or space) with the primary function of lipid capturing and delivery to the desired target site.[10,51]

In this study, we characterized *T. solium* FABPs *in silico* from the entire proteome using homology modeling. Molecular weight (13−15 kDa) was considered as the major criterion, and five TsMFABPs were identified in the entire proteome (Figure 1). Three novel putative proteins (TsM_000425500, TsM_000713700, and TsM_000802800) with the characteristic FABP structure and two proteins, TsM_001185100 (*TsMFABP1*) and TsM_000544100 (*TsMFABP2*), were already reported in literature (Figure 2). Although we have used a computational approach to identify the FABPs in *T. solium* proteome, here we have performed the FABP screening in the *T. solium* proteome four times to rule out the possibility of neglecting any possible FABP. We analyzed predicted FABPs for putative KEGG pathway function and their involvement in different cellular signaling cascades.[16] It was found that two proteins are involved in the PPAR-γ signaling pathway and regulation of lipogenesis in *T. solium* that is strongly correlated with the FABP function. Interestingly, predicting the FABP function in the regulation of PPAR-γ signaling and lipolysis suggests that lipid-mediated signaling is active in the *T. solium* parasite.

Comparison of all the protein sequences in multiple sequence alignment against different helminth FABPs and against human PMP2 protein depicted that TsM_000425500, TsM_000544100, and TsM_000713700 have some additional amino acid regions in their protein sequences, but the functional advantage of those regions is still unknown for the *T. solium* FABPs. We identified that all the genes were expressed at RNA levels, but only two (TsM_000544100 as *TsMFABP2* and TsM_001185100 as *TsMFABP1*) were expressed at the protein level (Figure 8A). They are antigenic in nature and known to be potential vaccine candidates in helminths. Previously, *Schistosoma mansoni* 14 kDa FABP induced predominant IgG response in mice, whereas *F. gigantica* FABP induced IgG1 response in mice and protected against *S. mansoni* infection.[52]

In another study, *F. hepatica* FABPs had shown cross-reactivity against IgGs *in vivo*.[47] Among all the IgGs, IgG1 is the most abundant and is found in enhanced levels after infection; it is involved in the protective responses and is also linked with the induction of type II immune responses.[53,54] During the asymptomatic phase of infection or the viable cyst infection, the parasite induces IgE and IgG1 response.[46] Therefore, we investigated whether the identified FABPs can form a stable interaction with IgG1. In the immune simulation, we identified that TsM_000425500 can possibly induce higher IgG responses than the other four proteins and can interact with the immune system. Among the IgG group, IgG1 was higher as compared to IgG2, and upon being docked with IgG1, TsM_000544100 and TsM_001185100 formed a stable complex. However, TsM_000425500 did not form a stable complex with the IgG1 Fab region. In this investigation, we purified TsM_001185100 (TsFABP1) protein using Ni-NTA

https://doi.org/10.1021/acsomega.3c09253
ACS Omega 2024, 9, 22557−22572

affinity chromatography and found that it is highly cross-reactive with NCC positive patients' serum samples in the EITB blot but not reactive with control or NCC negative serum samples (Figure 7A−C). This analysis suggested that these FABPs are antigenic in nature and make a stable complex with IgG1, which further suggests that these proteins can be targeted for future vaccine development. Previously, *F. gigantica* FABP was investigated for its diagnostic potential where the recombinant protein showed 94.87% specificity and 96.43% sensitivity; however, less than 10% of patients infected with other diseases (*S. mansoni* and ancylostomiasis) were also cross-reactive to *F. gigantica* FABP[55]These FABPs are secretory molecules and have high probability of interacting with the host-immune system and thus regulating the immune response. Previously, *T. solium* anti-hydrophobic ligand binding protein (HLBP) family member IgGs showed cross-reactivity against *Hymenolepis diminuta* HLBP, *Moniezia expansa*, and *Schistocephalus solidus*, suggesting that the structure of these proteins might be highly conserved across different species.[56] In another study, *T. solium* 14 and 18 kDa subunits of a larger protein complex (120 kDa) showed cross-reactivity against NCC patients' serum samples and were reliable for comparing the distinction between active NCC vs chronic NCC.[57] Altogether, FABPs, due to the high antigenicity and strong cross-reactivity against NCC positive patients' serum samples, can be used as potential diagnostic antigens.

As FABPs play a critical role in parasites' life cycle, we explored if they can be targeted as therapeutic agents that affect the viability of cysticerci. Previously, *Echinococcus multilocularis* FABP1−4 were explored as drug targets where FABP1, 3, and 4 showed strong binding with sulindac and clotrimazole and displaced ANS (FABP ligand) at 15 μM concentration; however, the ligand interacting residues were not identified.[58] A previous study of TsFABP1 and TsFABP2 indicates their role in retinol transport from the host to the parasite where such carrier system can be the drug target.[41] FABPs transport lipid ligands to the destination, and these proteins can facilitate the transport of lipophilic drug toward the parasites. *In silico* studies of *Echinococcus granulosus* FABP1 molecule provided an insight about the ligand conformation and ligand interacting amino acid residues that showed that the ligands interact with Arg107, Arg127, and Tyr129.[59] Interestingly, all the five FABPs expressed by *T. solium* interacted with the same ligands with different amino acids; however, Arg107, Arg127, and Tyr129 are the most common amino acids involved in ligand interaction. Additionally, Arg107, Arg127, and Tyr129 are also involved in ligand interaction in human FABP7, suggesting that both human and *T. solium* FABPs can bind to similar ligands.[60] In this case, *T. solium* FABPs may efficiently internalize the host lipid ligands and utilize them for growth and survival. We explored TsM_000544100 and TsM_001185100 (showed stability in the MD simulation) for ligand interacting residue identification. During the screening of the hydrophobic site or druggable site identification using sitemap, we screened the entire protein for all the sites, and interestingly, we identified the ligand-interacting site as the druggable site with the highest score. Here, we identified Arg107, Arg127, Tyr 129, and Arg140 as druggable amino acid residues and used them as drug targets, and we deduced the compounds β-nicotinamide mononucleotide (−40.73 kcal/mol) and enalaprilat dihydrate (−30.1 kcal/mol) against TsM_001185100 (TsMFABP1) and riboflavin (−52.9 kcal/mol) against TsM_000544100 (TsMFABP2) (Figure 8B,C). Among the three potential candidates, enalaprilat dihydrate showed the best cysticidal activity at 4 μg/mL (Figure 9A). However, β-nicotinamide mononucleotide showed effective cysticidal activity at 16 μg/mL (Figure 9A). These cysticidal activities showed the critical role of FABPs in the cysticercus life cycle where they are involved in fatty acid transport and participate in different signaling cascades.

TsFABP1 is the member of intracellular ligand binding protein (iLBP) superfamily in *T. solium*, involved in lipid uptake in the scolex region where it has preference toward palmitic acid and stearic acid.[8] In another study, *TsMFABP1* was detected extracellularly in the host system; in contrast, *TsMFABP2* was intracellularly restricted.[41] FABPs from helminth parasites were reported to be extensively involved in regulating the immune response of the host that facilitates parasite survival.[61] Apart from that, no clinically approved vaccine is available for mass vaccine administration against both cysticercosis and taeniasis that can effectively block parasite transmission across a population.[7] When considered collectively, our study suggests that FABPs have the potential to be desired candidates for vaccine development and as drug targets.

6. CONCLUSIONS

Our study identified all the FABPs of *T. solium* parasite. We also confirmed their presence as they are expressed at the RNA level in cysticercus stage, which causes the most severe form of infection to humans. *In silico* study of these FABPs with immunoglobulins suggested their interaction with IgG1 and their potential to act as strong immunogen, and they may be useful for developing a chimeric subunit vaccine in the future. Furthermore, ligand interacting sites were identified and targeted for potential cysticidal drug. Screening of DrugBank molecules against these sites gave some lead molecules; among them, enalaprilat dihydrate showed the most effective cysticidal activity, suggesting the critical role of TsM_001185100 in the parasite's life. Our study also highlights the need for extensive *in vivo* studies to critically validate the presence of these FABPs and establish them as potential therapeutic targets. In our current study, we have detected the RNA expression of all identified at the viable cysticercus stage; however, in future studies, more comprehensive studies can be performed to identify the role of these proteins at the protein level. Because these proteins are very critical to the parasites due to the lack of lipid biosynthesis machinery, establishing the role of FABPs will help us to understand the immunopathogenesis of NCC during the viable stage of the infection.

■ ASSOCIATED CONTENT

Supporting Information

The Supporting Information is available free of charge at https://pubs.acs.org/doi/10.1021/acsomega.3c09253.

List of primers used in the study; table of predicted FABPs in T. *solium* whole proteome; table showing localization of four proteins; list of amino acid residue positions on TsMFABPs that may be sensitive to phosphorylation; MMGBSA binding energies of complexes between predicted FABPs and IgG1-Fab region; figure of mapping of *T. solium* FABPs using EGGNOG; figure of relative amino acid conservation and mutation sensitive amino acids; figure of cellular localization and

https://doi.org/10.1021/acsomega.3c09253
ACS Omega 2024, 9, 22557−22572

transmembrane region prediction; figure of phosphorylation specific sites present in different TsMFABPs; molecular dynamics simulation study of FABPs; and TsMFABPs as antigens (PDF)

AUTHOR INFORMATION

Corresponding Author

Amit Prasad − *School of Biosciences and Bioengineering, Indian Knowledge System and Mental Health Centre, and Centre for Human-Computer Interaction, Indian Institute of Technology Mandi, Mandi, Himachal Pradesh 175005, India*; orcid.org/0000-0002-4235-9201; Email: amitprasad@iitmandi.ac.in

Authors

Suraj S. Rawat − *School of Biosciences and Bioengineering, Indian Institute of Technology Mandi, Mandi, Himachal Pradesh 175005, India*

Gagandeep Singh − *Dayanad Medical College and Hospital, Ludhiana, Punjab 141001, India*

Complete contact information is available at: https://pubs.acs.org/10.1021/acsomega.3c09253

Author Contributions

S.S.R. did the experiments. G.S. and A.P. deigned the project. S.S.R., G.S. and A.P. did data analysis. S.S.R. and A.P. drafted and critically evaluated the data and wrote the manuscript. All the authors read and approved the final manuscript for submission.

Notes

The authors declare no competing financial interest.

ACKNOWLEDGMENTS

C43 cells were a kind gift from Dr. Janesh Kumar, Senior Principal Scientist, Centre for cellular and Molecular Biology (CCMB), Hyderabad, India. S.S.R. acknowledges the Senior research fellowship from the Department of Biotechnology, Government of India, New Delhi. A.P. is supported through research grants from the Indian Council of Medical Research 92/03/2021-Omics/TF/MS and IIT Mandi iHub & HCI Foundation grant number IT MANDI iHub/RD/2023/0010.

DEDICATION

All work was completed after obtaining the necessary approval from the Institute Ethics Committee, Animal Ethics Committee (IIT/IAEC/2023/003), and Institute Biosafety Committee of IIT Mandi.

REFERENCES

(1) Nash, T. E.; Mahanty, S.; Loeb, J. A.; Theodore, W. H.; Friedman, A.; Sander, J. W.; Singh, G.; Cavalheiro, E.; Del Brutto, O. H.; Takayanagui, O. M.; et al. Neurocysticercosis: A natural human model of epileptogenesis. *Epilepsia* **2015**, *56* (2), 177−183.

(2) Nash, T. E.; Garcia, H. H. Diagnosis and treatment of neurocysticercosis. *Nat. Rev. Neurol* **2011**, *7* (10), 584−594.

(3) Gripper, L. B.; Welburn, S. C. Neurocysticercosis infection and disease-A review. *Acta Trop* **2017**, *166*, 218−224.

(4) Epidemiology, C.G. The World Health Organization 2030 goals for Taenia solium: Insights and perspectives from transmission dynamics modelling: CystiTeam Group for Epidemiology and Modelling of Taenia solium Taeniasis/Cysticercosis. *Gates Open Res.* **2019**, *3*, 1546.

(5) Arora, N.; Tripathi, S.; Sao, R.; Mondal, P.; Mishra, A.; Prasad, A. Molecular Neuro-Pathomechanism of Neurocysticercosis: How Host Genetic Factors Influence Disease Susceptibility. *Mol. Neurobiol* **2018**, *55* (2), 1019−1025. Prasad, K. N.; Prasad, A.; Verma, A.; Singh, A. K. Human cysticercosis and Indian scenario: a review. *J. Biosci* **2008**, *33* (4), 571−582. Singh, A. K.; Prasad, K. N.; Prasad, A.; Tripathi, M.; Gupta, R. K.; Husain, N. Immune responses to viable and degenerative metacestodes of Taenia solium in naturally infected swine. *Int. J. Parasitol* **2013**, *43* (14), 1101−1107.

(6) Kaur, R.; Arora, N.; Jamakhani, M. A.; Malik, S.; Kumar, P.; Anjum, F.; Tripathi, S.; Mishra, A.; Prasad, A. Development of multi-epitope chimeric vaccine against Taenia solium by exploring its proteome: an in silico approach. *Expert Rev. Vaccines* **2020**, *19* (1), 105−114.

(7) Kaur, R.; Arora, N.; Rawat, S. S.; Keshri, A. K.; Sharma, S. R.; Mishra, A.; Singh, G.; Prasad, A. Vaccine for a neglected tropical disease Taenia solium cysticercosis: fight for eradication against all odds. *Expert Rev. Vaccines* **2021**, *20* (11), 1447−1458.

(8) Illescas, O.; Carrero, J. C.; Bobes, R. J.; Flisser, A.; Rosas, G.; Laclette, J. P. Molecular characterization, functional expression, tissue localization and protective potential of a Taenia solium fatty acid-binding protein. *Mol. Biochem. Parasitol.* **2012**, *186* (2), 117−125.

(9) Rahman, M.; Lee, E. G.; Kim, S. H.; Bae, Y. A.; Wang, H.; Yang, Y.; Kong, Y. Characterization of hydrophobic-ligand-binding proteins of Taenia solium that are expressed specifically in the adult stage. *Parasitology* **2012**, *139* (10), 1361−1374.

(10) Alvite, G.; Esteves, A. Lipid binding proteins from parasitic platyhelminthes. *Front Physiol* **2012**, *3*, 363.

(11) Waterhouse, A.; Bertoni, M.; Bienert, S.; Studer, G.; Tauriello, G.; Gumienny, R.; Heer, F. T.; de Beer, T. A. P.; Rempfer, C.; Bordoli, L.; et al. SWISS-MODEL: homology modelling of protein structures and complexes. *Nucleic Acids Res.* **2018**, *46* (W1), W296−W303.

(12) Cantalapiedra, C. P.; Hernandez-Plaza, A.; Letunic, I.; Bork, P.; Huerta-Cepas, J. eggNOG-mapper v2: Functional Annotation, Orthology Assignments, and Domain Prediction at the Metagenomic Scale. *Mol. Biol. Evol.* **2021**, *38* (12), 5825−5829.

(13) Benet, L. Z.; Hosey, C. M.; Ursu, O.; Oprea, T. I. BDDCS, the Rule of 5 and drugability. *Adv. Drug Deliv Rev.* **2016**, *101*, 89−98.

(14) Schwede, T.; Kopp, J.; Guex, N.; Peitsch, M. C. SWISS-MODEL: An automated protein homology-modeling server. *Nucleic Acids Res.* **2003**, *31* (13), 3381−3385.

(15) Kelley, L. A.; Mezulis, S.; Yates, C. M.; Wass, M. N.; Sternberg, M. J. The Phyre2 web portal for protein modeling, prediction and analysis. *Nat. Protoc* **2015**, *10* (6), 845−858.

(16) Kanehisa, M.; Furumichi, M.; Tanabe, M.; Sato, Y.; Morishima, K. KEGG: new perspectives on genomes, pathways, diseases and drugs. *Nucleic Acids Res.* **2017**, *45* (D1), D353−D361.

(17) Gasteiger, E.; Gattiker, A.; Hoogland, C.; Ivanyi, I.; Appel, R. D.; Bairoch, A. ExPASy: The proteomics server for in-depth protein knowledge and analysis. *Nucleic Acids Res.* **2003**, *31* (13), 3784−3788.

(18) Howe, K. L.; Bolt, B. J.; Shafie, M.; Kersey, P.; Berriman, M. WormBase ParaSite - a comprehensive resource for helminth genomics. *Mol. Biochem. Parasitol.* **2017**, *215*, 2−10.

(19) Tamura, K.; Stecher, G.; Kumar, S. MEGA11: Molecular Evolutionary Genetics Analysis Version 11. *Mol. Biol. Evol.* **2021**, *38* (7), 3022−3027.

(20) Kaur, R.; Arora, N.; Rawat, S. S.; Keshri, A. K.; Singh, G.; Kumar, R.; Prasad, A. Recognition of immune reactive proteins as a potential multiepitope vaccine candidate of Taenia solium cysticerci through proteomic approach. *J. Cell Biochem* **2023**, *124*, 1587.

(21) Amit, P.; Prasad, K. N.; Kumar, G. R.; Shweta, T.; Sanjeev, J.; Kumar, P. V.; Mukesh, T. Immune response to different fractions of Taenia solium cyst fluid antigens in patients with neurocysticercosis. *Exp. Parasitol.* **2011**, *127* (3), 687−692.

(22) Nunez, G.; Villalobos, N.; Herrera, C. P.; Navarrete-Perea, J.; Mendez, A.; Martinez-Maya, J. J.; Bobes, R. J.; Fragoso, G.; Sciutto, E.; Aguilar, L.; et al. Anti-GK1 antibodies damage Taenia crassiceps

cysticerci through complement activation. *Parasitol Res.* **2018**, *117* (8), 2543−2553.
(23) Rio, D. C.; Ares, M.; Hannon, G. J.; Nilsen, T. W. Purification of RNA using TRIzol (TRI reagent). *Cold Spring Harb. Protoc* **2010**, *2010* (6), pdb.prot5439.
(24) Jumper, J.; Evans, R.; Pritzel, A.; Green, T.; Figurnov, M.; Ronneberger, O.; Tunyasuvunakool, K.; Bates, R.; Zidek, A.; Potapenko, A.; et al. Highly accurate protein structure prediction with AlphaFold. *Nature* **2021**, *596* (7873), 583−589.
(25) Pettersen, E. F.; Goddard, T. D.; Huang, C. C.; Couch, G. S.; Greenblatt, D. M.; Meng, E. C.; Ferrin, T. E. UCSF Chimera–a visualization system for exploratory research and analysis. *J. Comput. Chem.* **2004**, *25* (13), 1605−1612.
(26) Heo, L.; Park, H.; Seok, C. GalaxyRefine: Protein structure refinement driven by side-chain repacking. *Nucleic Acids Res.* **2013**, *41* (Web Serverissue), W384−W388.
(27) Laskowski, R.; Rullmann, J. A.; MacArthur, M.; Kaptein, R.; Thornton, J. AQUA and PROCHECK-NMR: programs for checking the quality of protein structures solved by NMR. *J. Biomol. NMR* **1996**, *8* (4), 477−486.
(28) Wiederstein, M.; Sippl, M. J. ProSA-web: interactive web service for the recognition of errors in three-dimensional structures of proteins. *Nucleic Acids Res.* **2007**, *35* (Web Server issue), W407−W410.
(29) Kall, L.; Krogh, A.; Sonnhammer, E. L. A combined transmembrane topology and signal peptide prediction method. *J. Mol. Biol.* **2004**, *338* (5), 1027−1036. Krogh, A.; Larsson, B.; von Heijne, G.; Sonnhammer, E. L. Predicting transmembrane protein topology with a hidden Markov model: application to complete genomes. *J. Mol. Biol.* **2001**, *305* (3), 567−580.
(30) Xue, B.; Dunbrack, R. L.; Williams, R. W.; Dunker, A. K.; Uversky, V. N. PONDR-FIT: a meta-predictor of intrinsically disordered amino acids. *Biochim. Biophys. Acta* **2010**, *1804* (4), 996−1010.
(31) Morris, G. M.; Huey, R.; Olson, A. J. Using AutoDock for ligand-receptor docking. *Curr. Protoc Bioinform.* **2008**, *Chapter 8*, 8−14.
(32) Weng, G.; Wang, E.; Wang, Z.; Liu, H.; Zhu, F.; Li, D.; Hou, T. HawkDock: a web server to predict and analyze the protein-protein complex based on computational docking and MM/GBSA. *Nucleic Acids Res.* **2019**, *47* (W1), W322−W330.
(33) Bhachoo, J.; Beuming, T. Investigating Protein-Peptide Interactions Using the Schrodinger Computational Suite. *Methods Mol. Biol.* **2017**, *1561*, 235−254.
(34) Arora, N.; Kaur, R.; Rawat, S. S.; Kumar, A.; Singh, A. K.; Tripathi, S.; Mishra, A.; Singh, G.; Prasad, A. Evaluation of Taenia solium cyst fluid-based enzyme linked immunoelectro transfer blot for Neurocysticercosis diagnosis in urban and highly endemic rural population of North India. *Clin. Chim. Acta* **2020**, *508*, 16−21.
(35) Kim, S.; Thiessen, P. A.; Bolton, E. E.; Chen, J.; Fu, G.; Gindulyte, A.; Han, L.; He, J.; He, S.; Shoemaker, B. A.; et al. PubChem Substance and Compound databases. *Nucleic Acids Res.* **2016**, *44* (D1), D1202−1213.
(36) Chile, N.; Clark, T.; Arana, Y.; Ortega, Y. R.; Palma, S.; Mejia, A.; Angulo, N.; Kosek, J. C.; Kosek, M.; Gomez-Puerta, L. A.; et al. In Vitro Study of Taenia solium Postoncospheral Form. *PLoS Negl Trop Dis* **2016**, *10* (2), No. e0004396.
(37) Ahmadian, M.; Suh, J. M.; Hah, N.; Liddle, C.; Atkins, A. R.; Downes, M.; Evans, R. M. PPARgamma signaling and metabolism: the good, the bad and the future. *Nat. Med.* **2013**, *19* (5), 557−566.
(38) Korbecki, J.; Bobinski, R.; Dutka, M. Self-regulation of the inflammatory response by peroxisome proliferator-activated receptors. *Inflamm Res.* **2019**, *68* (6), 443−458.
(39) Dai, M.; Yang, X.; Yu, Y.; Pan, W. Helminth and Host Crosstalk: New Insight Into Treatment of Obesity and Its Associated Metabolic Syndromes. *Front Immunol* **2022**, *13*, No. 827486.
(40) Tsai, I. J.; Zarowiecki, M.; Holroyd, N.; Garciarrubio, A.; Sanchez-Flores, A.; Brooks, K. L.; Tracey, A.; Bobes, R. J.; Fragoso, G.; Sciutto, E.; et al. The genomes of four tapeworm species reveal adaptations to parasitism. *Nature* **2013**, *496* (7443), 57−63.
(41) Kim, S. H.; Bae, Y. A.; Yang, H. J.; Shin, J. H.; Diaz-Camacho, S. P.; Nawa, Y.; Kang, I.; Kong, Y. Structural and binding properties of two paralogous fatty acid binding proteins of Taenia solium metacestode. *PLoS Negl Trop Dis* **2012**, *6* (10), No. e1868.
(42) Agellon, L. B. Importance of fatty acid binding proteins in cellular function and organismal metabolism. *J. Cell Mol. Med.* **2024**, No. e17703, DOI: 10.1111/jcmm.17703.
(43) Ramos-Benitez, M. J.; Ruiz-Jimenez, C.; Aguayo, V.; Espino, A. M. Recombinant Fasciola hepatica fatty acid binding protein suppresses toll-like receptor stimulation in response to multiple bacterial ligands. *Sci. Rep* **2017**, *7* (1), 5455.
(44) Vidarsson, G.; Dekkers, G.; Rispens, T. IgG subclasses and allotypes: from structure to effector functions. *Front Immunol* **2014**, *5*, 520.
(45) Parija, S. C.; Raman, G. A. Anti-Taenia solium larval stage Ig G antibodies in patients with epileptic seizures. *Trop Parasitol* **2011**, *1* (1), 20−25.
(46) Prodjinotho, U. F.; Lema, J.; Lacorcia, M.; Schmidt, V.; Vejzagic, N.; Sikasunge, C.; Ngowi, B.; Winkler, A. S.; Prazeres da Costa, C. Host immune responses during Taenia solium Neurocysticercosis infection and treatment. *PLoS Negl Trop Dis* **2020**, *14* (4), No. e0008005.
(47) Morphew, R. M.; Wilkinson, T. J.; Mackintosh, N.; Jahndel, V.; Paterson, S.; McVeigh, P.; Abbas Abidi, S. M.; Saifullah, K.; Raman, M.; Ravikumar, G.; et al. Exploring and Expanding the Fatty-Acid-Binding Protein Superfamily in Fasciola Species. *J. Proteome Res.* **2016**, *15* (9), 3308−3321.
(48) Loewenstein, Y.; Raimondo, D.; Redfern, O. C.; Watson, J.; Frishman, D.; Linial, M.; Orengo, C.; Thornton, J.; Tramontano, A. Protein function annotation by homology-based inference. *Genome Biol.* **2009**, *10* (2), 207.
(49) Kuhlman, B.; Bradley, P. Advances in protein structure prediction and design. *Nat. Rev. Mol. Cell Biol.* **2019**, *20* (11), 681−697.
(50) Dauter, Z.; Wlodawer, A. Progress in protein crystallography. *Protein Pept Lett.* **2016**, *23* (3), 201−210. Wlodawer, A.; Minor, W.; Dauter, Z.; Jaskolski, M. Protein crystallography for aspiring crystallographers or how to avoid pitfalls and traps in macromolecular structure determination. *FEBS J.* **2013**, *280* (22), 5705−5736.
(51) Furuhashi, M.; Hotamisligil, G. S. Fatty acid-binding proteins: role in metabolic diseases and potential as drug targets. *Nat. Rev. Drug Discov* **2008**, *7* (6), 489−503. Smathers, R. L.; Petersen, D. R. The human fatty acid-binding protein family: evolutionary divergences and functions. *Hum Genomics* **2011**, *5* (3), 170−191.
(52) Tang, C. L.; Zhang, R. H.; Liu, Z. M.; Jin, H.; He, L. Effect of regulatory T cells on the efficacy of the fatty acid-binding protein vaccine against Schistosoma japonicum. *Parasitol Res.* **2019**, *118* (2), 559−566. Rabia Aly, I.; Diab, M.; El-Amir, A. M.; Hendawy, M.; Kadry, S. Fasciola gigantica fatty acid binding protein (FABP) as a prophylactic agent against Schistosoma mansoni infection in CD1 mice. *Korean J. Parasitol.* **2012**, *50* (1), 37−43.
(53) Vaillant, A. A. J.; Jamal, Z.; Patel, P.; Ramphul, K. Immunoglobulin. *Stat. Pearls*; StatPearls Publishing **2023**.
(54) Pooley, H. B.; Begg, D. J.; Plain, K. M.; Whittington, R. J.; Purdie, A. C.; de Silva, K. The humoral immune response is essential for successful vaccine protection against paratuberculosis in sheep. *BMC Vet Res.* **2019**, *15* (1), 223.
(55) Amit, P.; Prasad, K. N.; Kumar, G. R.; Shweta, T.; Sanjeev, J.; Kumar, P. V.; Mukesh, T. Immune response to different fractions of Taenia solium cyst fluid antigens in patients with neurocysticercosis. *Exp Parasitol* **2011**, *127* (3), 687−692.
(56) Saghir, N.; Conde, P. J.; Brophy, P. M.; Barrett, J. A new diagnostic tool for neurocysticercosis is a member of a cestode specific hydrophobic ligand binding protein family. *FEBS Lett.* **2000**, *487* (2), 181−184.
(57) Lee, E. G.; Bae, Y. A.; Jeong, Y. T.; Chung, J. Y.; Je, E. Y.; Kim, S. H.; Na, B. K.; Ju, J. W.; Kim, T. S.; Ma, L.; Cho, S. Y.; Kong, Y.;

https://doi.org/10.1021/acsomega.3c09253
ACS Omega 2024, 9, 22557−22572

et al. Proteomic analysis of a 120 kDa protein complex in cyst fluid of Taenia solium metacestode and preliminary evaluation of its value for the serodiagnosis of neurocysticercosis. *Parasitology* **2005**, *131* (Pt 6), 867−879.
(58) Belgamo, J. A.; Alberca, L. N.; Porfido, J. L.; Romero, F. N. C.; Rodriguez, S.; Talevi, A.; Corsico, B.; Franchini, G. R. Application of target repositioning and in silico screening to exploit fatty acid binding proteins (FABPs) from Echinococcus multilocularis as possible drug targets. *J. Comput. Aided Mol. Des* **2020**, *34* (12), 1275−1288.
(59) Esteves, A.; Paulino, M. In silico studies of Echinococcus granulosus FABPs. *J. Biomol. Struct. Dyn.* **2013**, *31* (2), 224−239. Jakobsson, E.; Alvite, G.; Bergfors, T.; Esteves, A.; Kleywegt, G. J. The crystal structure of Echinococcus granulosus fatty-acid-binding protein 1. *Biochim. Biophys. Acta* **2003**, *1649* (1), 40−50.
(60) Hsu, H. C.; Tong, S.; Zhou, Y.; Elmes, M. W.; Yan, S.; Kaczocha, M.; Deutsch, D. G.; Rizzo, R. C.; Ojima, I.; Li, H. The Antinociceptive Agent SBFI-26 Binds to Anandamide Transporters FABP5 and FABP7 at Two Different Sites. *Biochemistry* **2017**, *56* (27), 3454−3462.
(61) Motran, C. C.; Silvane, L.; Chiapello, L. S.; Theumer, M. G.; Ambrosio, L. F.; Volpini, X.; Celias, D. P.; Cervi, L. Helminth Infections: Recognition and Modulation of the Immune Response by Innate Immune Cells. *Front Immunol* **2018**, *9*, 664.

https://doi.org/10.1021/acsomega.3c09253
ACS Omega 2024, 9, 22557−22572